

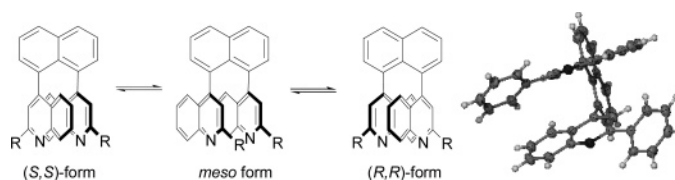
Synthesis and Stereodynamics of Highly Constrained 1,8-Bis(2,2'-dialkyl-4,4'-diquinolyl)naphthalenes (2)

Gilbert E. Tumambac and Christian Wolf*

Department of Chemistry, Georgetown University, Washington, D.C. 20057

cw27@georgetown.edu

Received September 10, 2004



Axially chiral 1,8-bis(2,2'-diphenyl-4,4'-diquinolyl)naphthalene, **8**, and 1,8-bis(2,2'-diisopropyl-4,4'-diquinolyl)naphthalene *N,N'*-dioxide, **9**, have been prepared to study the stereodynamics of these and other 1,8-diheteroarylnaphthalenes based on reversible first-order isomerization kinetics and crystallographic data. The ratio of the two enantiomeric *anti*-conformers to the meso *syn*-isomer of **8** and **9** was determined as 1.2:1 and 9.6:1. Investigation of the conformational stability of the atropisomers at enhanced temperatures using HPLC and NMR spectroscopy revealed a Gibbs activation energy of 122.4 (121.8) kJ/mol and 115.2 (109.0) kJ/mol for the *anti/syn*- (*syn/anti*)-isomerization of **8** and **9**, respectively. Comparison of the conformational stability of a series of 1,8-dipyridyl naphthalenes and 1,8-diquinolyl naphthalenes shows that the latter exhibit a significantly higher rotational energy barrier. While the *syn*- and *anti*-isomers of 1,8-dipyridyl naphthalenes interconvert rapidly at room temperature the stereoisomers of 1,8-diquinolyl naphthalenes can be isolated by chromatography or crystallization and stored at 25 °C for several months without any sign of racemization. The conformational stability of 1,8-diquinolyl naphthalenes is a consequence of significantly increased steric hindrance to isomerization in a highly congested T-shaped transition state. Conversion of 1,8-diheteroarylnaphthalenes to their corresponding *N,N'*-dioxides was found to result in an increased *anti/syn*-ratio and decreased rotational energy barrier, which was attributed to synergistic repulsive dipole/dipole interactions destabilizing the diastereomeric ground states and facilitated out-of-plane bending reducing the steric hindrance in the T-shaped transition state.

Introduction

Congested aromatic compounds have increasingly been employed in the design of organic materials and in the study of fundamental steric and electronic interactions such as π -stacking.¹ In particular, 1,8-disubstituted naphthalenes exhibiting alkyl,² aryl,³ and heteroaryl groups⁴ have been prepared to investigate the stability and structure of conformational isomers and transannular π - π interactions between adjacent aryl rings in the *peri* positions. Crystallographic analysis and computational studies of 1,8-diarylnaphthalenes have revealed that both *peri* aryl rings are cofacial and almost perpen-

dicular to the naphthalene ring in the ground state. The naphthalene moiety is slightly twisted and the two aryl substituents are splayed out to minimize steric interac-

(3) (a) House, H. O.; Magin, R. W.; Thompson, H. W. *J. Org. Chem.* **1963**, *28*, 2403–2406. (b) House, H. O.; Bashe, R. W. *J. Org. Chem.* **1965**, *30*, 2942–2947. (c) House, H. O.; Bashe, R. W. *J. Org. Chem.* **1967**, *32*, 784–791. (d) House, H. O.; Campbell, W. J.; Gall, M. *J. Org. Chem.* **1970**, *35*, 1815–1819. (e) House, H. O.; Koepsell, D. G.; Campbell, W. J. *J. Org. Chem.* **1972**, *37*, 1003–1011. (f) Clough, R. L.; Roberts, J. D. *J. Am. Chem. Soc.* **1976**, *98*, 1018–1020. (g) Pritchard, R. G.; Steele, M.; Watkinson, M.; Whiting, A. *Tetrahedron Lett.* **2000**, *41*, 6915–6918.

(4) (a) Zoltewicz, J. A.; Maier, N. M.; Fabian, W. M. F. *Tetrahedron* **1996**, *52*, 8703–8706. (b) Zoltewicz, J. A.; Maier, N. M.; Fabian, W. M. F. *J. Org. Chem.* **1996**, *61*, 7018–7021. (c) Maier, N. M.; Zoltewicz, J. A. *Tetrahedron* **1997**, *53*, 465–468. (d) Zoltewicz, J. A.; Maier, N. M.; Fabian, W. M. F. *J. Org. Chem.* **1997**, *62*, 2763–2766. (e) Zoltewicz, J. A.; Maier, N. M.; Fabian, W. M. F. *J. Org. Chem.* **1997**, *62*, 3215–3219. (f) Katoh, T.; Ogawa, K.; Inagaki, Y.; Okazaki, R. *Tetrahedron* **1997**, *53*, 3557–3570. (g) Zoltewicz, J. A.; Maier, N. M.; Lavieri, S.; Ghiviriga, I.; Abboud, K. A. *Tetrahedron* **1997**, *53*, 5379–5388.

(1) Jiang, J.; Lai, Y.-H. *J. Am. Chem. Soc.* **2003**, *125*, 14296–14297.

(2) (a) Fields, D. L.; Regan, T. H. *J. Org. Chem.* **1971**, *36*, 2986–2990. (b) Fields, D. L.; Regan, T. H. *J. Org. Chem.* **1971**, *36*, 2991–2995. (c) Fields, D. L.; Regan, T. H. *J. Org. Chem.* **1971**, *36*, 2995–3001.

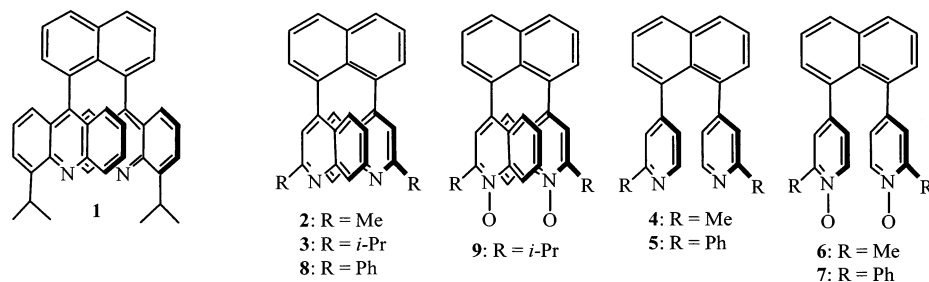
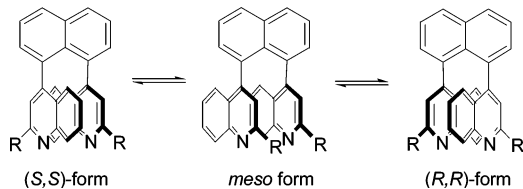


FIGURE 1. Structures of 1,8-diquinolyl- and 1,8-dipyridyl-naphthalenes.

SCHEME 1. Interconversion of the *syn*- and *anti*-Isomers of 1,8-Diquinolyl-naphthalenes



tions and through-space Coulomb repulsion. We have recently reported the preparation of highly congested 1,8-diacridyl-naphthalene **1** for metal-ion-selective and enantioselective sensing using fluorescence spectroscopy.⁵ As a consequence of the bulkiness of the cofacial acridyl moieties, no sign of rotation about the chiral acridyl-naphthalene axis of **1**, i.e., *syn/anti*-interconversion, has been observed even at very high temperature. Incorporation of significantly smaller substituents such as pyridyl or quinolyl rings into the *peri* positions of naphthalene affords diheteroaryl-naphthalenes **2–9** exhibiting a wide range of conformational stability, which may prove invaluable for the development of stereodynamic switches⁶ and sensors that can undergo induced isomerization in the presence of a chiral substrate.

We have recently reported the conformational stability and reversible first-order kinetics of 1,8-bis(2,2'-dimethyl-4,4'-diquinolyl)naphthalene, **2**, 1,8-bis(2,2'-diisopropyl-4,4'-diquinolyl)naphthalene, **3**, 1,8-dipyridyl-naphthalenes **4** and **5**, and the corresponding *N,N'*-dioxide derivatives **6** and **7**, Figure 1.⁷ Rotation about the heteroaryl-naphthalene bond of these congested atropisomers causes interconversion of the chiral *anti*-isomers to the *meso syn*-isomer via a T-shaped transition state exhibiting the edge of the rotating heteroaromatic ring directed toward the face of the neighboring ring. Rotation of one ring causes diastereomerization of the *anti*-isomer to the *syn*-isomer, i.e., the *meso syn*-conformer is the intermediate of the two enantiomeric *anti*-conformers, Scheme 1. As a consequence of the steric hindrance to rotation both 1,8-diquinolyl-naphthalenes **2** and **3** are conformationally stable at 25 °C but they undergo isomerization at elevated temperature. By contrast, the isomers of 1,8-

dipyridyl-naphthalenes **4–7** interconvert rapidly and cannot be isolated at room temperature. To further investigate the stereodynamics of congested 1,8-diheteroaryl-naphthalenes, we have prepared 1,8-bis(2,2'-diphenyl-4,4'-diquinolyl)naphthalene, **8**, and 1,8-bis(2,2'-diisopropyl-4,4'-diquinolyl)naphthalene *N,N'*-dioxide, **9**, and determined the Gibbs activation energy for *syn/anti*-isomerization, ΔG^\ddagger , of these atropisomers.

Results and Discussion

Following a synthetic strategy toward highly congested 1,8-disubstituted naphthalenes recently reported from our laboratories,⁵ we prepared 4-iodo-2-phenylquinoline, **11**, from commercially available 4-chloro-2-phenylquinoline, **10**, via acid promoted nucleophilic replacement of chloride by iodide. Lithiation of **11** using butyllithium at -78 °C and subsequent treatment with trimethylstannyl chloride afforded 2-phenyl-4-trimethylstannylquinoline, **12**. Stille cross-coupling of **12** and 1,8-dibromonaphthalene, **13**, gave 1,8-bis(2,2'-diphenyl-4,4'-diquinolyl)naphthalene, **8**, in 35% yield, Scheme 2.

The formation of **8** in 35% yield is quite remarkable since it requires two subsequent Pd-catalyzed cross-coupling steps of bulky stannane **12** at the adjacent *peri* positions of dibromonaphthalene **13**, Scheme 3. As a consequence of the high steric hindrance that can be expected during the second Stille cross-coupling cycle between intermediate 1-bromo-8-(2-phenylquinolyl)naphthalene, **14**, and stannane **12** competitive side reactions such as dehalogenation, methyl transfer during transmetalation and palladium C–H insertion reduce the overall yield.

The synthesis of **8** by Stille coupling affords a mixture of *syn*- and *anti*-isomers at thermal equilibrium because isomerization of atropisomers such as **8** exhibiting a 1,8-diquinolyl-naphthalene framework can be expected to occur fast under Stille coupling reaction conditions, *vide infra*. All attempts to prepare the *N,N'*-dioxide of **8** were not successful. However, treatment of 1,8-bis(2,2'-diisopropyl-4,4'-diquinolyl)naphthalene, **3**, with *m*-chloroperbenzoic acid gave *N,N'*-dioxide **9** in 75% yield.

The ratio of the two enantiomeric *anti*-conformers to the *syn*-conformer in hexanes/EtOH (85:15) at 97.8 °C was determined as 1.2:1 by HPLC analysis, whereas *N,N'*-dioxide **9** was found to exhibit an *anti/syn* ratio of 9.6:1 in DMSO at 100 °C.⁸ The observed ratio corresponds to a difference in Gibbs free energy of the *anti*- and *syn*-isomers, ΔG , of 1.6 kJ/mol for **8** and 4.9 kJ/mol for **9** according to the Boltzmann eq 1.⁹

$$n_1/2n_2 = \exp(-\Delta G^\circ/RT) \quad (1)$$

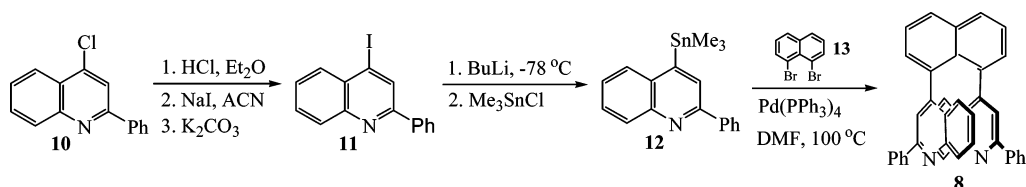
(5) (a) Wolf, C.; Mei, X. *J. Am. Chem. Soc.* **2003**, *125*, 10651–10658.

(b) Mei, X.; Wolf, C. *Chem. Commun.* **2004**, 2078–2079.

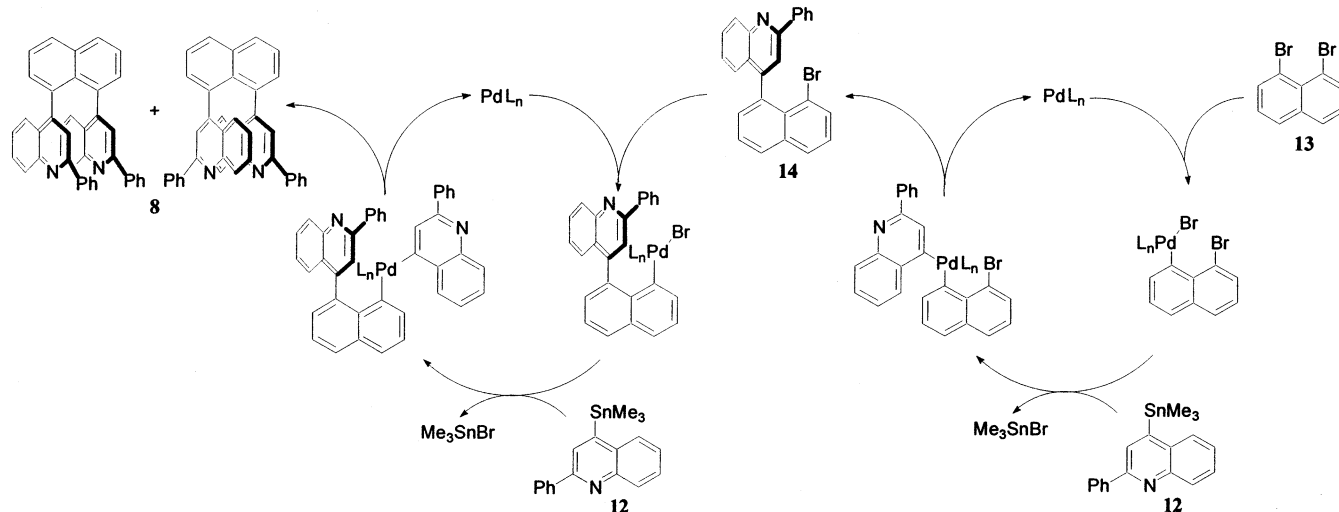
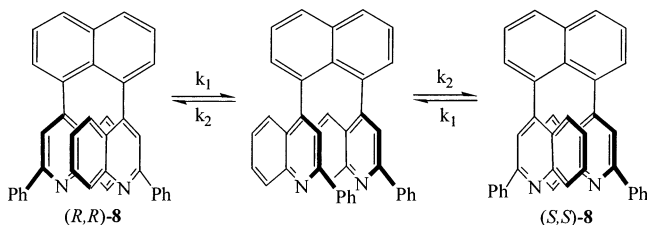
(6) (a) Feringa, B. L.; Van Delden, R. A.; Koumura, N.; Geertsema, E. M. *Chem. Rev.* **2000**, *100*, 1789–1816. (b) Bradford, R. F.; Schuster, G. B. *J. Org. Chem.* **2003**, *68*, 1075–1080.

(7) (a) Wolf, C.; Ghebremariam, B. T. *Synthesis* **2002**, 749–752. (b) Wolf, C.; Ghebremariam, B. T. *Tetrahedron: Asymmetry* **2002**, *13*, 1153–1156. (c) Wolf, C.; Tumambac, G. E. *J. Phys. Chem. A* **2003**, *107*, 815–817. (d) Tumambac, G. E.; Wolf, C. *J. Org. Chem.* **2004**, *69*, 2048–2055.

SCHEME 2. Synthesis of 1,8-Bis(2,2'-diphenyl-4,4'-diquinoyl)naphthalene, 8



SCHEME 3. Catalytic Cycles of the Pd-Catalyzed Stille Coupling of 12 and 13

SCHEME 4. Isomerization of the *syn*- and *anti*-Isomers of 8

We were pleased to find that the isomers of **8** can be separated by HPLC on a Whelk-O 1 column. Semi-preparative HPLC separation allowed us to determine individual response factors and to monitor the interconversion of the *syn*- and *anti*-isomers of **8** by chiral HPLC, Scheme 4.

To simplify the mathematical treatment of the interconversion of **8**, the rate constants k_1 and k_2 were determined based on a system of two nondistinguishable *anti*-conformers that isomerize via an intermediate *syn*-isomer following reversible first-order reaction kinetics, eq 2.

$$\frac{dx}{dt} = -2k_2(S_0 + x) + 2k_1(A_0 - x) \quad (2)$$

where $A_0 = [\textit{anti}\text{-}\mathbf{8a}]_0 = [\textit{anti}\text{-}\mathbf{8b}]_0$, $S_0 = [\textit{syn}\text{-}\mathbf{8}]$, k_1 = rate constant for *anti*- to *syn*-interconversion, k_2 = rate constant for *syn*- to *anti*-interconversion, $x = A_0 - A_t$ (concentration of A at time t), and $x_t = (-2k_2S_0 + 2k_1A_0)/[-2(k_2 + k_1)]e^{-2(k_2+k_1)t} + (2k_1A_0 - 2k_2S_0)/2(k_2 + k_1)$.

We found that the isolated isomers of **8** do not show any sign of interconversion at room temperature even after keeping them in solution for three months. Slow *syn/anti*-interconversion of **8** was observed at elevated

temperature and the diastereomerization and enantiomerization processes in hexanes/EtOH (85:15) at 97.8 °C were monitored by chiral HPLC at room temperature. Using eq 2, the rate constant for the *anti* → *syn*-isomerization, k_1 , was determined as 9.10×10^{-5} 1/s. The rate constant for the *syn* → *anti*-interconversion, k_2 , was calculated as 1.09×10^{-4} 1/s, Figure 2. The rotational energy barrier of **8** was determined according to the known equilibrium constant $K = k_1/k_2$ and the Eyring equation as 122.4 ± 0.2 (121.8) kJ/mol for the conversion of the *anti* (*syn*)- to the *syn* (*anti*)-isomer.

Since the diastereoisomers of N,N' -dioxide **9** exhibit different ^1H NMR spectra and can be separated by flash chromatography on silica gel, we decided to monitor the diastereomerization using purified *anti*-**9** by NMR spectroscopy in DMSO at 56.9 °C. Following the mathematical treatment described above, we determined the rate constant for the *anti* → *syn*-isomerization of **9**, k_1 , as 8.05×10^{-6} 1/s and the rate constant for the *syn* → *anti*-interconversion, k_2 , as 7.73×10^{-5} 1/s, Figure 3. The rotational energy barrier of **9** was calculated according to the known equilibrium constant $K = k_1/k_2$ and the Eyring equation as 115.2 ± 0.2 (109.0) kJ/mol for the conversion of the *anti* (*syn*)- to the *syn* (*anti*)-isomer.

The Gibbs activation energy, ΔG^\ddagger , for the diastereoisomerization of 1,8-dipyridynaphthalenes **4** and **5** and

(8) The *anti/syn*-ratio of the coupling product mixture of **8** was determined by chiral HPLC/UV analysis using a (*R,R*)-Whelk-O 1 column. Preparative HPLC separation of *anti*- and *syn*-isomers of **8** allowed us to determine the individual UV response factors of each atropisomer for quantification. The diastereomeric ratio of **9** was obtained by ^1H NMR spectroscopy. The determination of the *syn*- and *anti*-conformation of **8** and **9** was based on crystallographic analysis and on the successful separation of the enantiomers of the *anti*-isomer by chiral HPLC.

(9) The factor 2 in eq 1 accounts for the two enantiomeric *anti*-isomers of **8** and **9**.

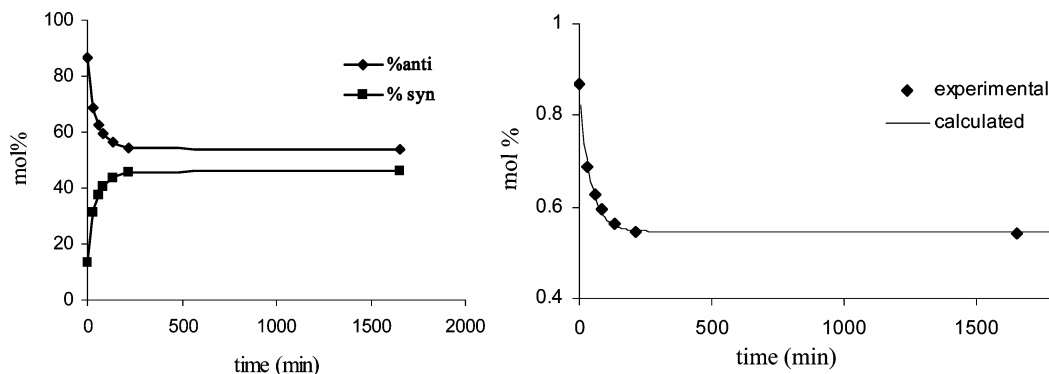


FIGURE 2. Plot of mol % of the *syn*- and *anti*-isomers (left) and curve fit as defined in eq 2 (right) for the reversible first-order isomerization of **8** at 97.8 °C.

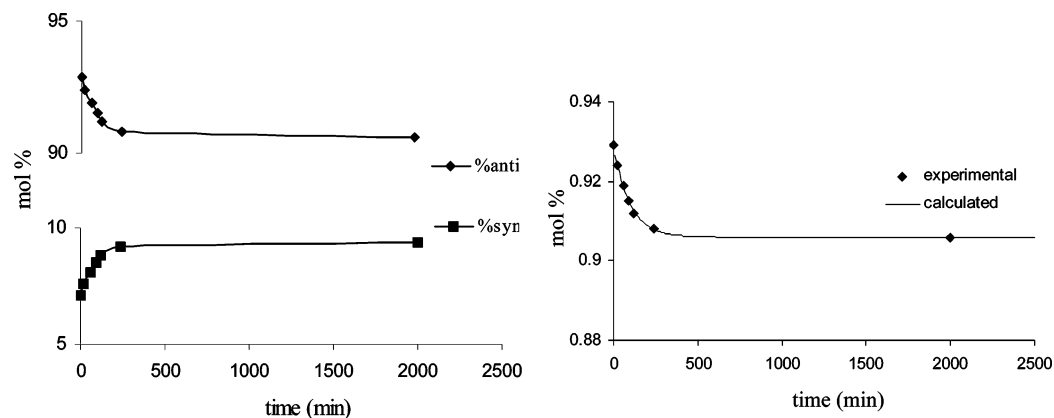
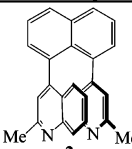
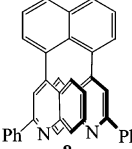
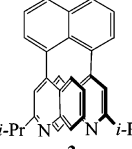
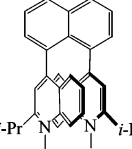


FIGURE 3. Plot of mol % of the *syn*- and *anti*-isomers (left) and curve fit as defined in eq 2 (right) for the reversible first-order isomerization of **9** at 56.9 °C.

TABLE 1. Isomerization Barrier of Atropisomers **2**, **3**, **8**, and **9**

entry	T [°C]	ΔG^\ddagger [kJ/mol] ^a
 2	71.0	116.0 +/-0.2 (112.1) ^b
 8	97.8	122.4 +/-0.2 (121.8) ^c
 3	66.2	117.2 +/-0.2 (111.1) ^d
 9	56.9	115.2 +/-0.2 (109.0) ^d

^a *anti*- to *syn*-isomerization (*syn*- to *anti*-isomerization). ^b In hexanes/EtOH (95:5). ^c In hexanes/EtOH (85:15). ^d In DMSO.

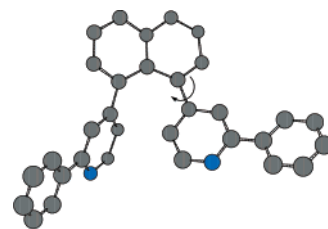


FIGURE 4. Favored T-shaped transition state of 1,8-bis(2,2'-diphenyl-4,4'-dipyridyl)naphthalene, **5**. Hydrogens are omitted for clarity.

their *N,N'*-dioxides **6** and **7** has previously been determined by variable-temperature NMR spectroscopy (DNMR) and dynamic HPLC and computer simulation (DHPLC).⁷ Exhibiting a rotational energy barrier of 64–73 kJ/mol the conformational isomers of the four 1,8-dipyridyl-naphthalene atropisomers interconvert rapidly and cannot be isolated at room temperature. Introduction of bulky quinolyl rings significantly impedes rotation about the chiral quinolyl–naphthyl axis resulting in Gibbs activation energy barriers above 110 kJ/mol for the *anti*/*syn*-interconversion of diquinolyl-naphthalenes **2**, **3**, **8**, and **9**. Accordingly, the *syn*- and *anti*-conformers of substituted diquinolyl-naphthalenes can be separated at room temperature and stored for more than 6 months without any sign of racemization. Isomerization of 2,2'-disubstituted 1,8-diheteroarylnaphthalenes **2–9** requires one aryl ring to rotate about the chiral axis. In the transition state, the edge of the rotating ring will

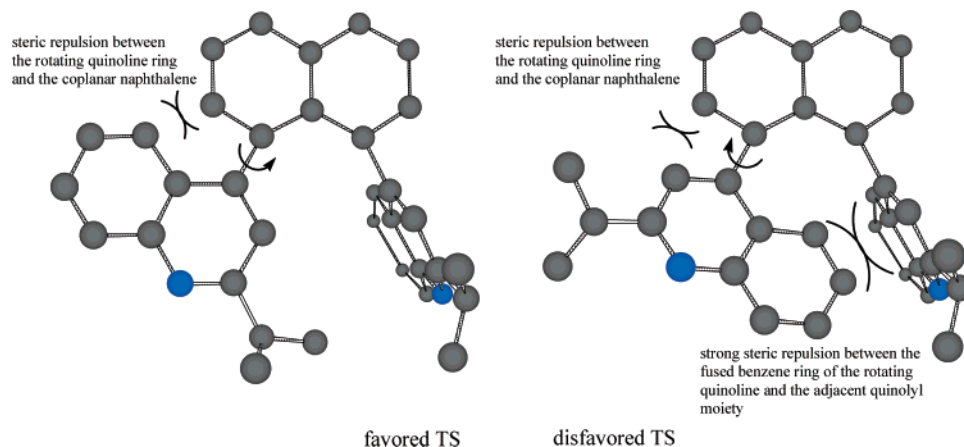


FIGURE 5. Possible T-shaped transition states of 1,8-bis(2,2'-diisopropyl-4,4'-diquinoyl)naphthalene, **3**, and steric repulsion experienced by the rotating quinoyl ring. The isopropyl group in position two of the rotating quinoline points toward (left) or away from (right) the adjacent quinoyl ring. All hydrogens are omitted for clarity.

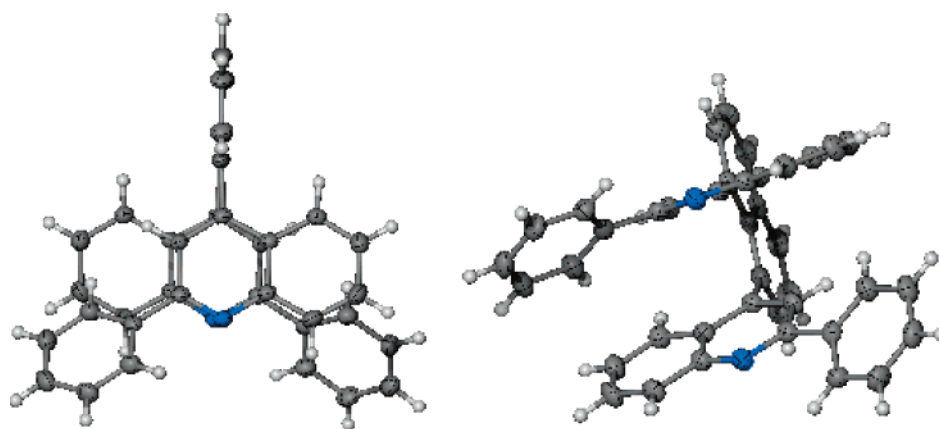


FIGURE 6. Single-crystal X-ray structures of **8**. The view along the naphthalene plane (left) shows the minimal twisting of the quinoyl rings. The side view (right) shows that the quinoyl rings are slightly splayed.

therefore be directed toward the adjacent heteroaryl moiety, which will remain perpendicular to the naphthalene plane albeit at increased splaying angle. This isomerization process can proceed via two T-shaped transition states exhibiting the substituent in position 2 of the pyridyl or the quinoyl ring of the rotating heteroaryl moiety either pointed toward or away from the other heteroaryl ring. Both heteroaryl rings will be significantly splayed away from each other in the transition state to minimize steric repulsion. For 1,8-dipyridyl-naphthalenes such as **5**, a T-shaped transition state exhibiting the 2-substituent of the rotating pyridyl ring pointing away from the other pyridyl ring has been considered less sterically hindered and therefore favored, Figure 4.^{7c}

This might not be the case with 1,8-diquinoylnaphthalenes. For example, the fused benzene moiety of the rotating quinoline of **3** would experience stronger steric repulsion by the adjacent quinoyl ring than the substituent in position 2, Figure 5. Isomerization is therefore likely to proceed via a transition state exhibiting the isopropyl group directed toward the adjacent quinoline albeit the fused benzene ring can be expected to undergo some steric interactions with the coplanar naphthyl ring.

While comparison of the conformational stability of 1,8-dipyridyl-naphthalenes and 1,8-diquinoylnaphthalenes

shows expected steric effects, a closer look reveals interesting electronic effects. As a consequence of differences in their intrinsic solubility, chromatographic and spectroscopic properties, and stereodynamics the isomerization of **2**, **3**, **8**, and **9** had to be investigated under different conditions. However, a comparison of the effect of *N*-oxidation on the conformational stability of diquinoylnaphthalene **3** and its *N,N*-dioxide **9** is possible as they have been investigated at similar temperatures in the same solvent. We found that *N*-oxidation of **3** slightly destabilizes the *syn*-isomer and reduces the energy barrier to *anti*-to-*syn*-isomerization from 117.2 kJ/mol to 115.2 kJ/mol, whereas the *syn*-to-*anti*-isomerization barrier is decreased from 111.1 to 109.0 kJ/mol. Based on the Boltzmann equation, the *anti*/*syn*-ratio of **3** and **9** has been calculated as 8.7 and 9.6, respectively.

To gain a better understanding of the structure and stereodynamics of 1,8-diheteroarylnaphthalenes we attempted to grow single crystals for crystallographic analysis. Isothermal vapor diffusion of diethyl ether into a dichloromethane solution of *anti*-**8** at room temperature gave a single crystal suitable for X-ray diffraction studies, Figure 6 and Table 2. Crystallographic analysis revealed that the single crystal is monoclinic and belongs to the *C2/c* space group. Because diastereomerization of **8** is

TABLE 2. Selected Crystallographic Data for **8**

empirical formula	C ₄₀ H ₂₆ N ₂
formula wt	534.66
crystal system	monoclinic
space group	C2/c
unit cell dimensions	$a = 18.885(2) \text{ \AA}$ $b = 10.3754(0) \text{ \AA}$ $c = 16.739(1) \text{ \AA}$ $\alpha = 90^\circ$ $\beta = 123.79(1)^\circ$ $\gamma = 90^\circ$
volume	2725.8 \AA ³
Z	4
density (calcd)	1.303 g cm ⁻³
crystal size	0.30 × 0.10 × 0.10 mm ³
N–N distance	4.24 \AA
splaying angle	10.0°
twisting angle	1.8°

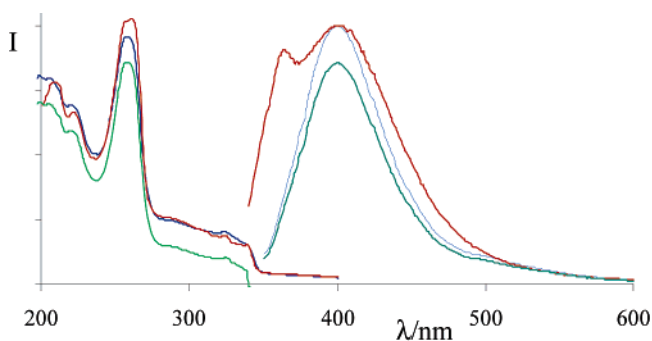


FIGURE 7. UV and fluorescence spectrum of 4-iodo-2-phenylquinoline, **11** (red line), *syn*-1,8-diquinolynaphthalene, **8** (green), and *anti*-**8** (blue) in acetonitrile. The concentration was 2.0×10^{-5} mol/L. Excitation wavelength was 330 nm.

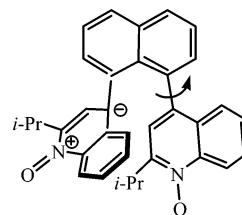
negligible under the crystallization conditions employed, the crystals did not show any presence of the *syn*-isomer. Interestingly, the solid-state structure of **8** shows splaying of 10.0° but almost no twisting of the antiparallel quinolyl rings.¹⁰ We know from our crystallographic experience with 1,8-diacridyl-naphthalenes and 1,8-diacridyl-naphthalene *N,N'*-dioxides that splaying of the heteroaryl groups is a common phenomenon for di-heteroaryl-naphthalenes, whereas additional twisting can only be observed with *N,N'*-dioxides and is probably a consequence of dipole–dipole repulsion.⁵

Despite the congested cofacial geometry of the quinolyl rings observed with **8** in the solid state, comparison of the UV and fluorescence spectra of monomeric 4-iodo-2-phenylquinoline, **11**, and the *syn*- and *anti*-isomers of 1,8-diquinolynaphthalene **8** shows no spectroscopic evidence for charge-transfer interactions and static excimer emission of **8** in solution, Figure 7. Similar results were obtained with 4-iodo-2-isopropylquinoline and **3**.

N,N'-Oxidation of diheteroaryl-naphthalene **3** increases the electron density in the cofacial aryl rings and is likely to affect the stability of both the ground and the transition state. We assume that the twisting commonly observed in diheteroaryl-naphthalene *N,N'*-dioxides is a

(10) Selected crystallographic data for **8**: formula C₄₀H₂₆N₂, M = 534.66, crystal dimensions 0.3 × 0.1 × 0.1 mm³, monoclinic, space group C2/c, $a = 18.885(2) \text{ \AA}$, $b = 10.3754(0) \text{ \AA}$, $c = 16.739(1) \text{ \AA}$, $\alpha = \gamma = 90^\circ$, $\beta = 123.79(1)^\circ$, $V = 2725.8 \text{ \AA}^3$, $Z = 4$, $\rho_{\text{calcd}} = 1.303 \text{ g cm}^{-3}$, $2\theta_{\text{max}} = 54.0^\circ$, $T = 187 \text{ K}$, 3186 independent reflections ($R_{\text{int}} = 2.59\%$), of which 2477 were above $4\sigma(F)$. $R1 = 0.051$, $wR2 = 0.1161$ with $I > 2\sigma(I)$, $R\sigma = 0.0247$, $\text{Goof} = 1.135$, $\Delta\rho_{\text{max}} = 0.25 \text{ e \AA}^{-3}$, $\Delta\rho_{\text{min}} = -0.21 \text{ e \AA}^{-3}$.

SCHEME 5. Electron-Donating Effect of the *N*-Oxide Function of **9** Increasing the Electron Density at the Carbon of the Pivotal Aryl–Aryl Bond and Thus Facilitating Out-of-Plane Bending and Isomerization



consequence of destabilizing dipole–dipole interactions between the parallel heteroaryl *N*-oxide moieties. These destabilizing interactions will be less prominent in **3** than in its *N,N'*-dioxide derivative **9** and should be more effective in the ground state than in the T-shaped transition state.¹¹ Accordingly, *N*-oxidation can be expected to reduce the rotational energy barrier of 1,8-diheteroaryl-naphthalenes because the enhanced dipole–dipole repulsion between the *N*-oxide moieties is likely to reduce the stability of the diastereomeric ground states. *N*-Oxidation can also be expected to affect the stability of the transition state as has previously been reported with axially chiral biphenyls.¹² The introduction of electron-donating groups into the para positions of axially chiral 2,2'-bis(trifluoromethyl)biphenyls was found to increase the enantiomerization rate of these atropisomers. In accordance with IR spectroscopy measurements of aromatic compounds performed by Kross and co-workers,¹³ the rate increasing effect of electron-donating groups was attributed to increased electron density at the pivotal carbon atoms of the phenyl–phenyl bond, which facilitates out-of-plane bending of one aryl moiety in the coplanar transition state of interconverting biphenyls. By contrast, incorporation of electron-withdrawing groups into the para positions of biphenyls was found to decrease the rate of enantiomerization of biphenyls because out-of-plane bending is impeded in these cases. Similarly, conversion of the quinolyl rings of **3** to *N*-oxides will enhance the electron density at the pivotal quinolyl carbon atom attached to the naphthalene ring and is therefore expected to facilitate out-of-plane bending of one quinolyl moiety and rotation of the adjacent quinoline ring, Scheme 5.

Since the chemical shift of a carbon atom is directly related to its electron density, the ¹³C NMR shifts of the pivotal quinolyl carbons of 4-iodo-2-isopropylquinoline, **15**, and 4-iodo-2-isopropylquinoline *N*-oxide, **16**, and of the corresponding diquinolynaphthalenes **3** and **9** were determined by HMBC and HMQC NMR experiments. In both cases *N*-oxidation results in a significant upfield shift of most carbon atoms including the carbon atom in para position to the quinolyl nitrogen. Oxidation of **15** to **16** causes an upfield shift of this carbon atom from

(11) Cozzi, F.; Cinquini, M.; Annunziata, R.; Dwyer, T.; Siegel, J. S. *J. Am. Chem. Soc.* **1992**, *114*, 5729–5733.

(12) (a) King Ling, C. C.; Harris, M. M. *J. Chem. Soc.* **1964**, 1825–1835. (b) Oki, M.; Yamamoto, G. *Bull. Chem. Soc. Jpn.* **1971**, *44*, 266–270. (c) Wolf, C.; König, W. A.; Roussel, C. *Liebigs Ann.* **1995**, 781–786. (d) Wolf, C.; Hochmuth, D. H.; König, W. A.; Roussel, C. *Liebigs Ann.* **1996**, 357–363.

(13) Kross, R. D.; Fassel, V. A.; Margoshes, M. *J. Am. Chem. Soc.* **1956**, *78*, 1332–1335.

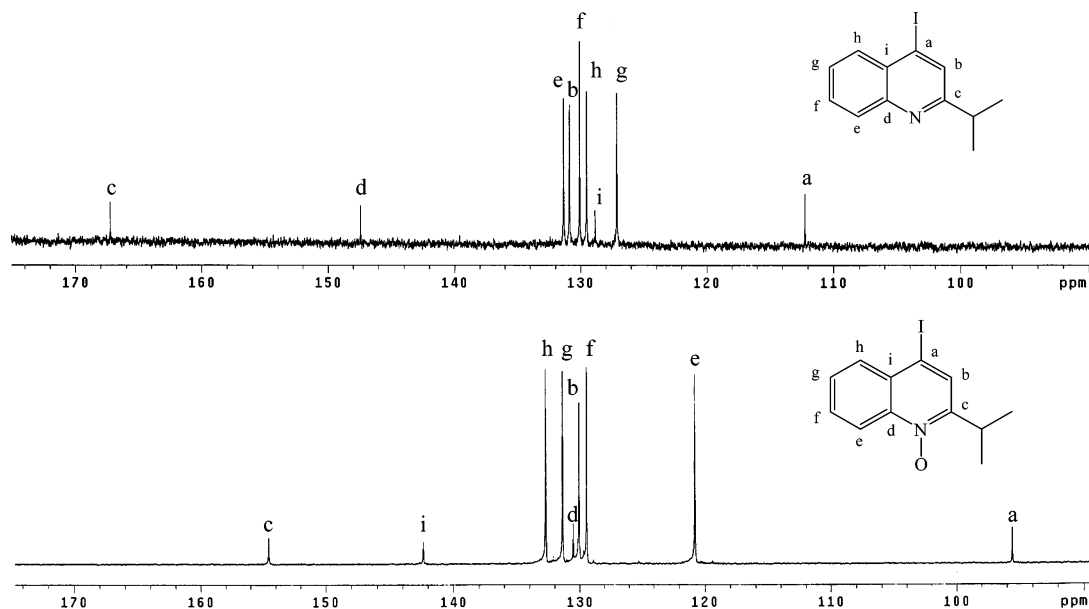


FIGURE 8. Assignment of aromatic ^{13}C NMR signals of 4-iodo-2-isopropylquinoline, **15** (top), and its *N*-oxide, **16** (bottom).

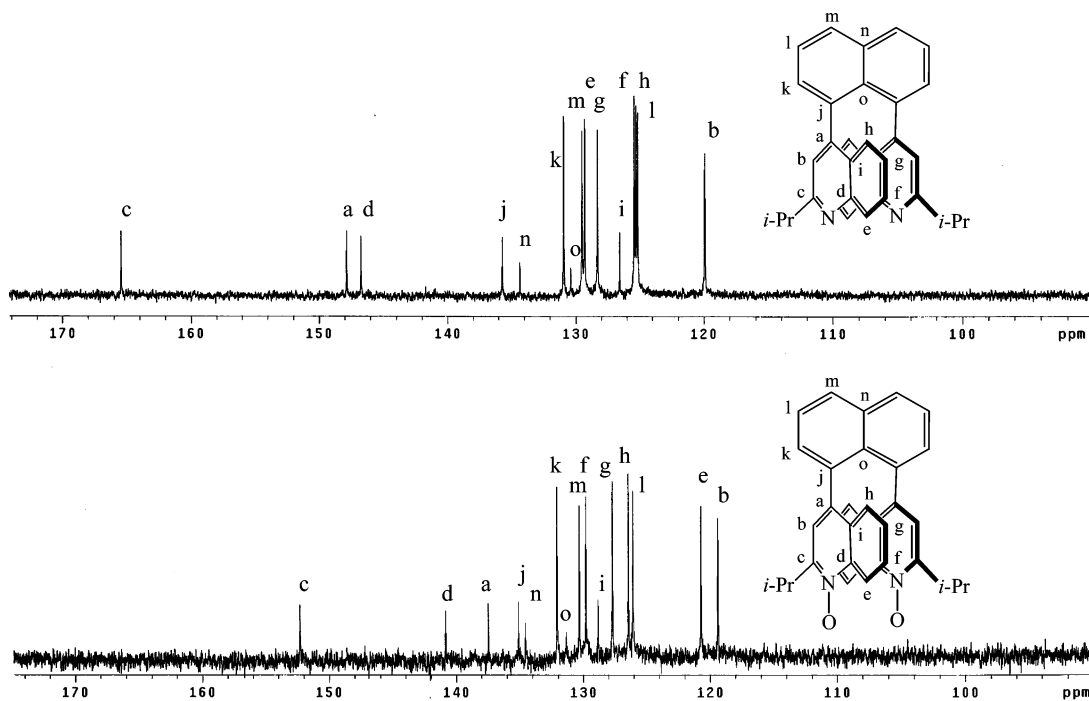


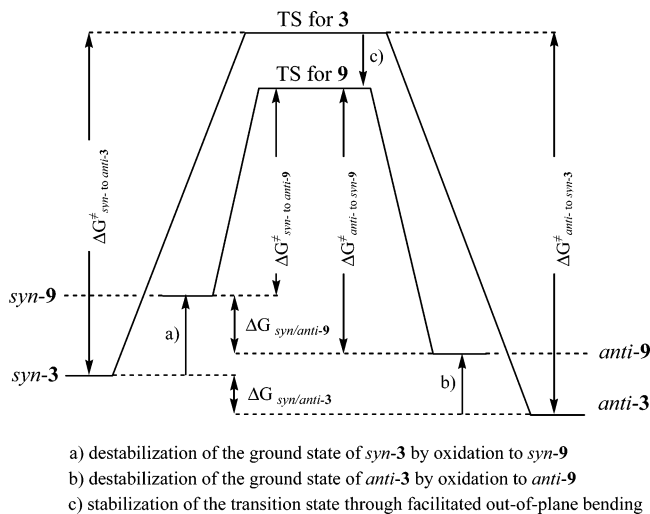
FIGURE 9. Assignment of aromatic ^{13}C NMR signals of *anti*-1,8-bis(2,2'-diisopropyl-4,4'-diquinolyl)naphthalene, **3** (top), and its *N,N'*-dioxide, **9** (bottom).

112.2 to 95.6 ppm, see (C)-a in Figure 8. Comparison of the corresponding ^{13}C NMR shifts in **9** and **3** shows an upfield shift from 147.9 to 137.5 ppm, Figure 9. Because the same trend is found in the simple quinolyl iodides **15** and **16**, the change in chemical shifts observed upon oxidation of **3** to **9** cannot be fully explained by the anisotropic ring current of the adjacent quinolyl ring but must be at least partially attributed to increased π -electron density at the quinolyl carbon bonded to the naphthyl ring.

Our ^{13}C NMR experiments thus show increased electron density at the pivotal quinolyl carbon atoms due to *N*-oxidation of diquinolyl naphthalene **3**, which is ex-

pected to facilitate vibrational out-of plane bending.¹³ In accordance with the kinetic studies performed with substituted biphenyls mentioned above, one can expect less steric interactions in the T-shaped transition state of diheteroarylnaphthalene *N,N'*-dioxides such as **9**. Accordingly, at least two electronic effects on the conformational stability as a result of *N*-oxidation of diheteroarylnaphthalenes have to be considered, i.e., a decrease in the rotational stability of diheteroarylnaphthalenes because of dipole–dipole destabilization of the ground state and reduced steric hindrance in the transition state due to facilitated out-of-plane bending, Scheme 6.

SCHEME 6. Illustration of the Destabilization of the Ground and Stabilization of the Transition State Due to *N*-Oxidation of Diheteroarylnaphthalene **3 to *N,N'*-Dioxide **9** and the Resulting Decrease in the Rotational Energy Barrier**



Conclusion

Because of the significant steric hindrance to rotation about the heteroaryl–naphthyl bond in the T-shaped transition state the *syn*- and *anti*-isomers of 1,8-diquinolyl-naphthalenes can be isolated at room temperature, whereas 1,8-dipyridyl-naphthalenes undergo rapid isomerization. *N*-Oxidation of diheteroarylnaphthalenes was found to increase the isomerization rate albeit electronic effects on the barrier to rotation of these atropisomers are significantly smaller than steric effects. The reduced rotational energy barrier of *N,N'*-dioxides was attributed to two synergistic effects on the relative stability of the ground and transition states. Kinetic investigations and crystallographic analysis suggest that repulsive dipole/dipole interactions between the coplanar rings of 1,8-diheteroarylnaphthalene *N,N'*-dioxides selectively destabilize the ground state and thus decrease the conformational stability. In addition, *N*-oxidation results in increased electron density at the pivotal carbon atoms facilitating out-of-plane bending and rotation about the axially chiral naphthyl–quinolyl bond via a less sterically hindered transition state.

Experimental Section

All commercially available reagents, solvents, and 2-phenyl-4-chloroquinoline, **10**, were used without further purification. 1,8-Dibromonaphthalene was prepared from 1,8-diaminonaphthalene as described in the literature.¹⁴ The synthesis of 1,8-bis(2,2'-diisopropyl-4,4'-diquinolyl)naphthalene, **3**, 4-iodo-2-isopropylquinoline, **15**, and 4-iodo-2-isopropylquinoline *N*-oxide, **16**, has been described previously.^{7d} All reactions were carried out under nitrogen atmosphere and under anhydrous conditions. Organostannanes are highly toxic and should only be used in a vented hood and when wearing eye and skin protection. Products were purified by flash chromatography on SiO₂ (particle size 0.032–0.063 mm). GC-MS was performed on a Fison Instruments MD800 mass spectrometer equipped

with a gas chromatograph using a 15 m DB-1 column. Atmospheric pressure chemical ionization (APCI) mass spectra were collected on a YMC-Pack CN column (4.6 × 250 mm²) using an HPLC/MSD system equipped with electrospray and atmospheric pressure chemical ionization MS detection and hexanes/EtOH = 9:1 as the mobile phase. All analytical and preparative HPLC separations of **8** were conducted using a (*R,R*)-Whelk-O 1 column (4.6 × 250 mm²) and hexanes/EtOH = 85:15 as the mobile phase at a flow rate of 1 mL/min and UV detection at 254 nm. Preparative separations were performed by repetitive injections of 100 μL of **8** dissolved in hexanes/EtOH = 1:1 at a concentration of approximately 20 mg/mL. For analytical separations, **8** was dissolved in the same diluent at a concentration of 1 mg/mL and 10 μL was injected. The HPLC selectivity factor, α , for the enantioseparation of **8** was determined as 1.14. NMR spectra were obtained at 300 MHz (¹H NMR) and 75 MHz (¹³C NMR) using CDCl₃ as the solvent. Chemical shifts are reported in ppm relative to TMS.

All kinetic experiments of **8** were conducted in a closed vessel designed for high-pressure experiments using a concentration of 1 mg/mL of **8** in hexanes/EtOH = 85:15. The vessel was submerged in an ethylene glycol bath and the temperature was measured using a calibrated digital thermometer. The samples were cooled to room temperature prior to analysis by HPLC using a (*R,R*)-Whelk-O 1 column (4.6 × 250 mm²) and hexanes/EtOH = 85:15 as the mobile phase. Because one enantiomer was found to coelute with the *syn*-diastereoisomer, individual response factors of the *anti*- and *syn*-isomers of **8** purified by preparative HPLC or crystallization were determined for quantitation. The individual response factors in hexanes/EtOH = 85:15 at 254 nm were calculated as 2256 A units/ug (*anti*-**8**) and 862 A units/ug (*syn*-**8**). Kinetic studies of **9** were conducted at a concentration of 1 mg/mL in deuterated DMSO using NMR spectroscopy. The temperature of the sample was allowed to equilibrate for 10 min prior to the first NMR experiment. Integration of well-resolved signals of the *anti*- and *syn*-isomers of **9** allowed us to monitor the diastereomerization process. The NMR temperature was measured following a procedure reported by Merbach et al.¹⁵ All isomerization reactions investigated followed reversible first-order kinetics.

Single-crystal X-ray diffractions of **8** were collected at –86 °C using a Siemens platform diffractometer with graphite monochromated Mo K α radiation ($\lambda = 0.71073$ Å). The structures were solved by direct methods and refined with full-matrix least-squares/difference Fourier analysis using SHELX-97-2 software. Non-hydrogen atoms were refined with anisotropic displacement parameters and all hydrogen atoms were placed in calculated positions and refined with a riding model. Data were corrected for the affects of absorption using SADABS.

4-Iodo-2-phenylquinoline (11).¹⁶ To a solution of 4-chloro-2-phenylquinoline **10** (4.0 g, 16.7 mmol) in 20 mL of THF was added 2 M HCl in ether (10.0 mL, 20.0 mmol). After 5 min, the solvent was removed and the precipitate dried under reduced pressure. The hydrochloride salt and NaI previously dried at 120 °C under vacuum (25.5 g, 0.17 mol) were suspended in 150 mL of anhydrous acetonitrile and refluxed for 24 h. After cooling to room temperature, an aqueous solution of 10% K₂CO₃ and 5% NaHSO₃ (20 mL) was added. After the mixture was extracted with CH₂Cl₂, the combined organic layers were dried over MgSO₄ and the solvents were evaporated under reduced pressure. The residue was chromatographed on silica gel (100:20:1 hexanes:ethyl acetate:triethylamine as the eluent) to give **11** (4.4 g, 80%) as a yellow oil.

¹H NMR: δ 7.45–7.56 (m, 3H), 7.60 (ddd, $J = 1.4$ Hz, $J = 7.0$ Hz, $J = 8.3$ Hz, 1H), 7.75 (ddd, $J = 1.4$ Hz, $J = 7.0$ Hz, $J = 7.0$ Hz, 1H).

(15) Ammann, C.; Meier, P.; Merbach, A. E. *J. Magn. Reson.* **1982**, *46*, 319–321.

(16) Wolf, C.; Tumambac, G. E.; Villalobos, C. N. *Synlett* **2003**, 1801–1804.

(14) Seyferth, D.; Vick, S. C. *J. Organomet. Chem.* **1977**, *141*, 178–187.

= 8.5 Hz, 1H), 8.02 (ddd, $J = 0.5$ Hz, $J = 1.4$ Hz, $J = 8.3$ Hz, 1H), 8.10 (ddd, $J = 0.5$ Hz, 1.4 Hz, 8.5 Hz, 1H), 8.13–8.16 (m, 2H), 8.50 (s, 1H). ^{13}C NMR: δ 112.5, 127.5, 127.7, 128.8, 129.1, 129.6, 130.2, 130.4, 130.5, 131.3, 137.9, 147.7, 156.9. EI-MS (70 eV): 331 (64, M^+), 204 ($\text{M}^+ - \text{I}$), 126 (4, $\text{M}^+ - \text{I} - \text{C}_6\text{H}_5 - \text{H}$).

2-Phenyl-4-trimethylstannylquinoline (12). A solution of *n*-butyllithium (9.2 mL, 1.6 M in hexanes) was added dropwise to a solution of 4-iodo-2-phenylquinoline (**11**) (4.0 g, 12.0 mmol) in anhydrous diethyl ether at -78 °C. The mixture was allowed to stir for 30 min and a solution of Me_3SnCl in hexanes (18.0 mL, 1.0 M) was added. The reaction mixture was allowed to warm to room temperature and was stirred for another 8 h. The reaction was quenched with 10% NH_4OH . Extraction with CH_2Cl_2 , drying of the combined organic layers over MgSO_4 , and evaporation of the solvent were followed by purification by flash chromatography (mobile phase: 100:10:1 hexanes:ethyl acetate:triethylamine) to afford **12** (2.5 g, 57%) as a viscous yellow oil. GC-MS analysis revealed the presence of small amounts of 2-phenylquinoline impurities that could not be separated by chromatography. The material was therefore used for the preparation of **8** without further purification.

^1H NMR: δ 0.52 (s, 9H), 7.46–7.56 (m, 4H), 7.71 (ddd, $J = 1.4$ Hz, $J = 6.9$ Hz, $J = 8.4$ Hz, 1H), 7.78 (ddd, $J = 0.6$ Hz, $J = 1.4$ Hz, $J = 8.1$ Hz, 1H), 8.00 (s, 1H), 8.12–8.15 (m, 2H), 8.18 (ddd, $J = 0.6$ Hz, $J = 1.4$ Hz, $J = 8.4$ Hz, 1H). ^{13}C NMR: δ -7.6, 126.6, 128.1, 128.2, 128.3, 129.4, 129.5, 129.6, 130.0, 131.4, 132.0, 133.2, 140.6, 148.0, 155.3, 156.1. EI-MS (70 eV): m/z (%) 369 (28, M^+), 354 (100, $\text{M}^+ - \text{Me}$), 324 (48, $\text{M}^+ - 3\text{Me}$), 204 (78, $\text{M}^+ - \text{Me}_3\text{Sn}$), 177 (10, $\text{M}^+ - \text{Me}_3\text{Sn} - \text{HCN}$).

1,8-Bis(2,2'-diphenyl-4,4'-diquinolyl)naphthalene (8). A solution of 1,8-dibromonaphthalene (0.30 g, 1.02 mmol), 132 mg of $\text{Pd}(\text{PPh}_3)_4$, and CuO (0.30 g, 3.9 mmol) in 15 mL of anhydrous DMF was stirred at 100 °C under N_2 . After 5 min, 2-phenyl-4-trimethylstannylquinoline (**12**) (1.5 g, 4.1 mmol) in 5 mL of DMF was added. The reaction was stirred for 13 h at 140 °C, cooled to room temperature, and quenched with 10% NH_4OH . The aqueous layer was extracted with diethyl ether. The combined organic layers were washed with H_2O , dried over MgSO_4 , and concentrated under vacuum. Purification by flash chromatography (hexanes:ethyl acetate:triethylamine) yielded **8** (182 mg, 35%) as a yellow oil.

^1H NMR of *anti*-isomer: δ 6.90 (s, 2H), 7.08–7.28 (m, 6H), 7.27–7.37 (m, 8H), 7.51–7.54 (m, 4H), 7.61–7.70 (m, 4H), 8.17 (dd, $J = 1.4$ Hz, $J = 8.3$ Hz, 2H). ^{13}C NMR of *anti*-isomer: δ 120.1, 120.4, 125.6, 125.7, 126.9, 128.7, 129.5, 129.7, 129.8, 129.9, 130.7, 131.3, 131.4, 132.6, 134.7, 136.0, 147.1, 148.3, 165.8. ^1H NMR of *syn*-isomer: δ 6.82 (ddd, $J = 1.4$ Hz, $J =$

6.9 Hz, $J = 8.3$ Hz, 2H), 6.97 (d, $J = 7.5$ Hz, 2H), 7.08–7.28 (m, 4H), 7.27–7.37 (m, 6H), 7.41 (dd, $J = 1.4$ Hz, $J = 7.0$ Hz, 2H), 7.51–7.54 (m, 2H), 7.61–7.70 (m, 4H), 6.97 (d, $J = 7.5$ Hz, 2H), 8.17 (dd, $J = 1.4$ Hz, $J = 8.3$ Hz, 2H). ^{13}C NMR of *syn*-isomer: δ 119.9, 120.2, 125.5, 125.7, 127.7, 127.9, 128.6, 128.9, 129.0, 129.3, 129.6, 129.9, 130.1, 131.3, 135.1, 147.1, 149.0, 165.8. LC-APCI-MS: m/z (%) 535 [100, ($\text{M} + \text{H}$) $^+$]. Anal. Calcd for $\text{C}_{40}\text{H}_{26}\text{N}_2$: C, 89.86; H, 4.90; N, 5.24. Found: C, 89.52; H, 4.78; N, 5.04.

1,8-Bis(2,2'-diisopropyl-4,4'-diquinolyl)naphthalene *N,N'*-Dioxide (9). To a solution of **3** (100 mg, 0.2 mmol) in ether (10.0 mL) at 0 °C was added dropwise a solution of *m*-CPBA (170 mg, 1.0 mmol) in THF. After stirring for 30 min, the reaction mixture was allowed to come to room temperature and stirred for 16 h. The solvent was removed, followed by neutralization with an aqueous solution of K_2CO_3 . The aqueous layer was then extracted with CH_2Cl_2 . After drying of the combined methylene chloride extracts over MgSO_4 and removal of the solvent, the crude residue was purified by flash chromatography using 30:1 hexanes:EtOH as the eluent to give **9** (80 mg, 75%) as white crystals.

^1H NMR of *anti*-isomer: δ 0.67 (d, $J = 6.9$ Hz, 6H), 0.94 (d, $J = 6.9$ Hz, 6H), 3.49 (sept, $J = 6.9$ Hz, 2H), 6.42 (s, 2H), 7.26 (m, 6H), 7.63 (m, 4H), 8.16 (d, $J = 8.0$ Hz, 2H), 8.66 (d, $J = 8.8$ Hz, 2H). ^{13}C NMR of *anti*-isomer: δ 19.2, 19.8, 28.2, 119.4, 120.8, 126.1, 126.4, 127.8, 128.9, 129.8, 130.4, 131.3, 132.1, 134.5, 135.1, 137.5, 140.9, 152.2. ^1H NMR of *syn*-isomer: δ 1.21 (d, $J = 6.9$ Hz, 6H), 1.29 (d, $J = 6.9$ Hz, 6H), 3.81 (sept, $J = 6.9$ Hz, 2H), 6.72–6.75 (m, 2H), 6.82 (s, 2H), 6.83–6.86 (m, 2H), 7.91–7.94 (m, 4H), 8.01–8.03 (m, 4H), 8.39–8.41 (m, 2H). ^{13}C NMR of *syn*-isomer: δ 19.2, 19.8, 28.2, 120.0, 120.4, 120.5, 120.8, 126.0, 126.3, 129.9, 130.3, 131.7, 132.2, 135.3, 152.4. LC-APCI-MS: 499 [($\text{M} + \text{H}$) $^+$]. Anal. Calcd for $\text{C}_{24}\text{H}_{30}\text{N}_2\text{O}_2$: C, 81.90; H, 6.06; N, 5.62. Found: C, 82.39; H, 6.43; N, 5.37.

Acknowledgment. We gratefully acknowledge the National Science Foundation for financial support (CAREER Award CHE 0347368). We thank Leah B. Casabianca for help with HMQC and HMBC NMR experiments.

Supporting Information Available: Crystallographic data for the single-crystal structure of **8**, kinetic studies and mathematical treatment of the isomerization of **8** and **9**, and HMBC and HMQC spectra of **3**, **9**, **15**, and **16**. This material is available free of charge via the Internet at <http://pubs.acs.org>.

JO048399N